Computer Simulation of Systemic Circulation and Clot Lysis Dynamics During Thrombolytic Therapy That Accounts for Inner Clot Transport and Reaction

Sriram Anand, PhD; Scott L. Diamond, PhD

Background We developed a computer model to predict lysis rates of thrombi for intravenous thrombolytic regimens based on the convective/diffusive penetration of reacting and adsorbing fibrinolytic species from the circulation into the proximal face of a dissolving clot.

Methods and Results Solution of a one-compartment plasma model provided the dynamic concentrations of fibrinolytic species that served as inlet conditions for simulation of the one-dimensional spatiodynamics within a dissolving fibrin clot of defined composition. The model predicted the circulating levels of tissue plasminogen activator (TPA) and plasminogen levels found in clinical trials for various intravenous therapies. To test the model predictions under in vitro conditions, plasma clots were perfused with TPA (0.1 μmol/L) and plasminogen (1.0 μmol/L) delivered at constant permeation velocity of 0.1 or 0.2 mm/min. The model provided an accurate prediction of the measured lysis front movement. For TPA administration regimens used clinically, simulations predicted clot dissolution rates that were consistent with observed reperfusion times. For unidirectional permeation, the continual accumulation of adsorbing species at the moving lysis front due to prior rounds of solubilization and rebinding was predicted to provide for a marked concentration of TPA and plasmin and the eventual depletion of antiplasmin and macroglobulin in an advancing ($\approx$0.25 mm thick) lysis zone.

Conclusions Pressure-driven permeation greatly enhances and is a primary determinant of the overall rate of clot lysis and creates a complex local reaction environment at the plasma/clot interface. With simulation of reaction and transport, it becomes possible to quantitatively link the administration regimen, plasminogena activator properties, and thrombolytic outcome. (***Circulation*. 1996;94:763-774.**)

Key Words • fibrinolysis • hemodynamics • pharmacokinetics • plasminogen activators • thrombolysis

Intravenous thrombolytic therapy for the treatment of acute MI is conducted in accordance with a specific administration regimen. Depending on the regimen and plasminogen activator(s) used, a set of events (plasminogen activation, inhibition, clearance) determines the constituents of the circulation that come in contact with the occlusive thrombus. Species in the plasma adjacent to the clot can penetrate into the proximal face of the clot via diffusion and pressure-driven permeation. The effects of pressure-driven permeation have been studied in vitro[1-5] and in vivo[6-8] and indicate thrombolysis is diffusion limited unless transport by pressure-driven permeation is present. Accurate prediction of thrombolytic outcome must account for both the biochemical kinetics and penetration rates of proteins in dissolving thrombi.

Arterial thrombi within the coronary artery are $\approx$1 cm long.[9] With intravenous administration, plasminogen activators within the systemic circulation are carried efficiently to the nearest unobstructed coronary bifurcation upstream of the clot. If the clot is close to this unobstructed bifurcation, the clot is initially in direct contact with the well-mixed systemic circulation. If the clot is centimeters downstream of an unobstructed bifurcation, then recirculating secondary flows are responsible for delivery of plasminogen activators to the clot. In this case, time lags and inefficient transport coupling may occur between the pharmacodynamics of the systemic circulation and lytic events at the clot. At the proximal face of the clot, thrombolytic therapy is a process characterized by the convective/dispersive penetration of enzymes that bind the erodible fibrin fibers of the blood clot.[4,5,10] Protease transport involves the binding of proteins to the fibrin fiber network with subsequent solubilization of these enzymes back into the interstitial fluid of the clot.[5]

In the present study, we coupled the calculation of the dynamics in the circulation with the spatiotemporal transport/reaction phenomena that occur within a dissolving thrombus. In these simulations, clot lysis rate is a direct and quantitative result of (1) the biochemistry of the circulation, (2) the properties and administration regimen of the thrombolytic agent, (3) the physical structure and biochemical composition of the thrombus, and (4) the local pressure environment. Using simulation and in vitro experimentation, we showed that increases in permeation lead to direct increases in the rate of plasma clot lysis. The simulation provided the tool with which to understand reaction and transport in a coupled manner as these two processes occur in vivo. The agreement between simulations and in vitro plasma clot lysis indicates that fibrinolysis is quantifiable despite its reaction complexity. With continually improving measurements of clot composition, permeability, and reaction kinetics, computer simulation can serve as a useful

Received November 28, 1995; revision received February 1, 1996; accepted February 3, 1996.

From the Bioengineering Laboratory, Department of Chemical Engineering, The State University of New York at Buffalo.

Correspondence to Dr Scott L. Diamond, Bioengineering Laboratory, Department of Chemical Engineering, The State University of New York, Buffalo, NY 14260. E-mail sdiamond@eng.buffalo.edu.

Selected Abbreviations and Acronyms

AP = α_2-antiplasmin
FDP = fibrin degradation products
LAD = left anterior descending coronary artery
MI = myocardial infarction
PAI-1 = plasminogen activator inhibitor type I
PPP = platelet-poor plasma
TPA = tissue plasminogen activator
uPA = urokinase plasminogen activator

predictive tool for the evaluation of new agents and therapeutic approaches.

Methods

Plasma Clot Lysis Under Conditions of Permeation

Human venous blood was collected with anticoagulation (final concentration of 0.38% wt/vol sodium citrate) through venipuncture of healthy, nonsmoking volunteers (who gave informed consent) in accordance with the guidelines and approval of the Internal Review Board of the State University of New York at Buffalo. Platelet-rich plasma (obtained through centrifugation of whole blood at 150*g* for 15 minutes) was further centrifuged at 1900*g* for 15 minutes to yield PPP. Small aliquots of recalcified PPP were promptly suctioned to the midpoint of a 1-mL polystyrene sterile pipette to form individual 2-cm-long PPP clots. At 4 hours after coagulation, a lytic cocktail containing 0.1 μmol/L recombinant human TPA (Activase, Genentech Inc) and 1.0 μmol/L human Glu-plasminogen (American Diagnostica, Inc) diluted in 0.05 mol/L Tris-HCl, pH 7.4, 0.1 mol/L NaCl, and 5 mmol/L $CaCl_2$ was backfilled adjacent to each PPP clot. A Harvard syringe pump with multiple syringes was then used to perfuse the solutions into the clots at constant velocity of 0.1 or 0.2 mm/min. The position of the lysis front was recorded with time over the course of the experiment. All experiments were conducted on a microscope stage maintained at 37°C with an airstream incubator.

Theory

Intravenous thrombolytic administration regimens for acute MI involve a combination of bolus and continuous infusions. In the circulation, changes in blood chemistry occur due to fibrin-independent plasminogen activation. To describe these changes in the circulation, we calculated the concentration of each species (C_i, μmol/L) through the solution of a set of coupled ordinary differential equations. The differential equation used to model the rate of change of concentration of each species (C_i) in plasma is given in Equation 1. The plasma of the circulation was treated as a single, well-mixed compartment that can receive a user-specified infusion regimen for any species, $I_i(t)$ (μmol/s), and any species may be eliminated at a given rate by clearance, $K_i(t)$. This algorithm represents a generalized approach that is consistent with earlier pharmacodynamic models of thrombolytic therapy.[11]

$$(1)\quad V_{plasma}\frac{dC_i}{dt}=V_{plasma}\sum_j\sum_k R^i(C_j,C_k)+I_i(t)-K_i(t)$$

The reaction network treated in the present study is shown in Fig 1, where fibrin is present only in the clot and is not present in the circulation. In the circulation, the fibrin of Fig 1 is replaced by a nonspecific soluble cofactor for fibrin-independent TPA-mediated plasminogen activation. This fibrin-independent activation of plasminogen by TPA is neglected in the clot and is not shown in Fig 1 because that reaction is slow compared with fibrin-dependent activation. Since fibrinogen, degradation products, and other factors in blood can serve as cofactors for this reaction, the rate constants for fibrin-independent TPA-mediated plasminogen activation in the circulation are lumped and apparent. This approach captures to some extent the evolving role of FDP in the circulation in a time-averaged manner. We have used the activation kinetics of Glu-plasminogen by TPA in the absence of fibrin[12] as the apparent Michaelis-Menten kinetic constants (K_m=28 μmol/L, k_2=0.3 s^{-1}) as originally proposed by Tiefenbrunn et al[11] for TPA-mediated plasminogen activation in plasma. In the circulation, the rate of generation (or loss) of the *i*th species $R^i(C_j,C_k)$ was determined by the reaction between the *j*th and *k*th species. Reaction rate expressions may be of any form, typically Michaelis-Menten or second-order association kinetics, as shown in Fig 1 (without fibrin) and Table 1. The clearance rate of each species, K_i, is taken as a first-order process in C_i determined from the half-life of the species where $K_i=(k\cdot C_i\cdot V_{plasma})$. The circulatory half-lives of TPA and uPA (two-chain) were taken as 5 and 60 minutes, respectively.[13,14] Nominal plasma levels of the various fibrinolytic species (Table 2) were used as the initial conditions for the solution of the set of ordinary differential equations for the 12 soluble species shown in Fig 1. The calculated dynamic levels of

Nomenclature

c_i = free phase concentration of *i*th species based on fluid phase volume, μmol/L
C_i = systemic concentration of *i*th species based on total plasma volume, μmol/L
D_i^{eff} = effective diffusion coefficent of *i*th species in fibrin, cm^2/s
D_L = longitudinal dispersion coefficient, cm^2/s
D_{pore} = pore diameter, cm
$I_i(t)$ = time-dependent infusion regimen of *i*th species, $\mu mol\cdot s^{-1}$
k = specific permeability, cm^2
k'' = second-order association rate, $\mu mol\cdot L^{-1}\cdot s^{-1}$
k_2 = Michaelis-Menten kinetic rate constant, s^{-1}
k_{cat} = kinetic rate constant for fibrin-bound protease, s^{-1}
$K_i(t)$ = time-dependent clearance rate of *i*th species, $\mu mol\cdot s^{-1}$
K_m = Michaelis constant, μmol/L
$k_{f,i}^r$ = forward rate coefficient of *i*th species associating with *r*th site in solid phase, $\mu mol\cdot L^{-1}\cdot s^{-1}$
$k_{r,i}^r$ = reverse rate coefficient of *i*th species dissociating from *r*th site in solid phase, s^{-1}
L = historic amount of lysis based on fibrin phase volume, μmol/L
L_T = total length of fiber in gel
M_W = molecular weight
N_{av} = Avogodro's number
q_r = number of *r*th binding sites per monomer
R_f = fiber radius, nm
R_{fo} = initial fiber radius, nm
R_{jk}^i = generation of *i*th species in fluid phase by interaction of *j* and *k* species, $\mu mol\cdot L^{-1}\cdot s^{-1}$
s_i = bound concentration of *i*th species based on fibrin fiber volume, μmol/L
${}^sR_{jk}^i$ = generation of *i*th species in solid phase by interaction of *j* and *k* species, $\mu mol\cdot L^{-1}\cdot s^{-1}$
t = time, s
v = convective velocity within the pore, cm/s
V_T = total volume of the clot
v_x = convective velocity component in the axial direction within pore
$\bar{v}$ = superficial velocity, cm/s
x = axial position, cm
ϵ = porosity of bed
ϵ_{fiber} = porosity of fiber
ξ_{rj} = interaction parameter allowing binding of *j*th species binding to *r*th site
γ = solubilization parameter (equivalent moles solubilized/moles of cleavages)
θ_r = total *r*th binding site concentration based on solid phase volume, μmol/L
ρ = density of fibrin gel, mg/cm^3
ρ_{fiber} = density of fiber, mg/cm^3

species within the circulation then served as inlet conditions for prediction of local clot lysis dynamics (Fig 2).

At the clot, fibrinolysis is a multicomponent reaction network with fluid-phase reaction as well as heterogeneous reactions catalyzed by species within the fibrin fiber phase (Fig 1). The rates for reaction and adsorption steps are based on in vitro assays[4,5] and are shown in Table 1. For transport of species in eroding fibrin, the instantaneous concentration of a soluble species at some position in the fluid phase of the fibrin gel is described with the use of Equation 2. The rate of change of the local volume-averaged concentration of a species in the fluid phase depends on the net adsorption rate to the fibrin fibers, dispersion, permeation, homogeneous reaction in the free phase, and the effects due to change of volume of the solid phase as species are released during solubilization of the solid-phase and free-phase species are diluted to a small extent in the lost fibrin fiber volume.[5] The rate of change of a fibrin-bound concentration of the ith species depends on the rate of binding, dissociation, and heterogeneous reaction (Equations 3 and 4), where the jth species may compete for the rth binding site (ξ_{rj}=one interaction; ξ_{rj}=no interaction).

$$\epsilon\frac{\partial c_i}{\partial t}=(s_i-c_i)\frac{\partial \epsilon}{\partial t}-(1-\epsilon)\frac{\partial N_i^T}{\partial t}+\nabla\cdot[D\cdot\nabla(\epsilon c_i)] \quad (2)$$

Rate of change of c_i | Gain due to lysis | Net adsorption to fibrin | Diffusion/dispersion

$$-\nabla\cdot(\epsilon c_i v)+\epsilon\sum_1\sum_k R_{1k}{}^i$$

Permeation | Homogeneous reaction

$$\frac{\partial N_i^T}{\partial t}=k_{f,i}{}^r c_i(\theta_r-\sum_j \xi_{rj}s_j)-k_{r,i}{}^r(s_i) \quad (3)$$

Net adsorption to fibrin | Adsorption | Desorption

$$\frac{\partial s_i}{\partial t}=\frac{\partial N_i^T}{\partial t}+\sum_1\sum_k {}^sR_{1k}{}^i \quad (4)$$

Rate of chance of s_i | Rate of transfer | Heterogeneous reaction

The permeation term in Equation 2 reduces to $\bar{v}(\partial c/\partial x)$ for one-dimensional flow, where the superficial velocity for pressure-driven permeation through fibrin is described by Darcy's law as $\bar{v}=k/\mu(\Delta P/L)$ where k is the specific permeability and μ is the viscosity of the permeating plasma.[5] Equations 2 through 4 for each species in Fig 1 are solved for specified initial conditions $c_i(x,0)$ and $s_i(x,0)$ on the clot domain $0<x<L_{clot}$. Danckwerts inlet and outlet boundary conditions were used for the solution of the partial differential equations (Equations 5 and 6), where $C_i^{inlet}(t)=C_i(t)$ from Equation 1.

$$\bar{v}C_i^{inlet}(t)=\left(\bar{v}c_i-D_L\frac{\partial c_i}{\partial x}\right)\Bigg|_{x=0} \quad (5)$$

$$\left.\frac{\partial c_i}{\partial x}\right|_{x=L}=0 \quad (6)$$

The effective diffusion (D_i^{eff}) of proteins in the fluid space of the fibrin network due to brownian motion is not significantly hindered.[15,16] Hydrodynamic dispersion (brownian diffusion plus micromixing) will occur during pressure-driven permeation, and this process scales with the velocity in the pore space (v_x) and the pore diameter (D_{pore}) as correlated[17] in Equation 7 for the dispersion coefficient D_L. The specific permeability of fibrin was based on the fiber diameter and gel porosity according to the Davies equation[18] (Equation 8).

$$D_L=D_i^{eff}+D_{pore}v_x \quad (7)$$

$$k=\frac{D_{fiber}{}^2}{70(1-\epsilon)^{3/2}[1+52(1-\epsilon)^{3/2}]} \quad (8)$$

In eroding fibrin, it is necessary to relate the proteolysis rate with evolving material properties (D_{fiber}, ϵ, k). Through evaluation at all

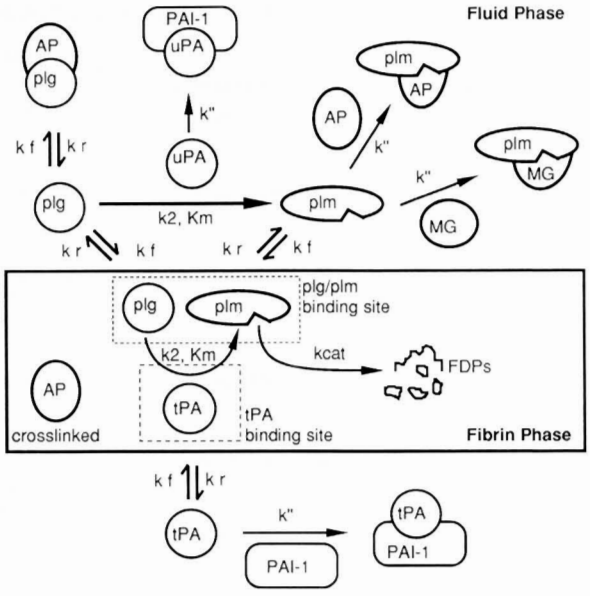

FIG 1. Summary of the fibrinolytic reaction pathway. Plasminogen (plg) is activated to plasmin (plm) in the fluid phase by urokinase (uPA), whereas fibrin-bound plg is activated TPA in the fibrin phase. The free-phase plm is inhibited by AP and macroglobulin (MG), whereas the bound-phase plm is protected from inhibition. The uPA and TPA are inhibited in the free phase by PAI-1. Inhibition reactions were assumed to be irreversible. Soluble species can reversibly adsorb and desorb with fibrin under kinetically controlled conditions. The plg and plm compete for the same sites on the intact fibrin monomer, whereas TPA binds a unique site. All kinetic constants for reversible adsorption and enzymatic reaction are given in Table 1. Single-chain to two-chain conversions of TPA and uPA as well as conversions of Glu-plasmin(ogen) to Lys-plasmin(ogen) were not considered.

times of the instantaneous rate of cutting within the fiber [$k_{cat}\cdot s_{plasmin}$, [μmol/L per second]] at some location x', it is possible to calculate the historic amount of cutting within the fiber (μmol/L of cleavages) made at x' and t'. In defining a solubilization factor γ that relates the number of equivalent monomers solubilized to the number of cleavages made, the amount of solubilization or lysis ($L[x',t']$, μmol/L of fibrin lysed at x' and t') from the solid phase can be defined as a function of the historic amount of cuts made by plasmin at position x' (Equation 9). For fibrin, the solubilization factor has been estimated to be a constant with a value of 0.1. This corresponds to the estimate that for every 10 cleavages by plasmin, an equivalent of one subunit of fibrin is solubilized.[19]

$$L(x',t')=\gamma\int_0^{t'} k_{cat}s_{plasmin}(x',t)dt \quad (9)$$

The local plasmin concentration in the fiber and the solubilization rate are formulated with respect to a volume average within the solid fiber volume. Plasmin gradients within the fiber are not calculated. Details for the calculation of the fiber properties during lysis are given in "Appendix 1." The solution of Equations 1 through 4 with initial conditions and boundary conditions is described in "Appendix 2."

Results

Predicting Circulation Dynamics During Intravenous Thrombolytic Therapy

Calculation of systemic concentrations during thrombolytic therapy was required for predictions of local clot lysis. We simulated intravenous administration regimens to predict dynamic TPA and plasminogen levels in the circulating plasma in humans. The prediction of systemic

TABLE 1. Adsorption and Catalytic Rate Constants of Fibrinolysis

	Kinetic Constants	Reference
Reversible adsorption		
$fbn+plg^f \rightleftharpoons plg^b$	K_d=38 μmol/L	Lucas et al[24]
	k_f=1.087×10^{-4} μmol·L^{-1}·s^{-1}	2.0 sites/monomer
	k_r=4.131×10^{-3}·s^{-1}	
$fbn+plm^f \rightleftharpoons plm^b$	K_d=0.5 μmol/L	Thorsen et al[51]
	k_f=0.5×10^{-3} μmol·L^{-1}·s^{-1}	2.0 sites/monomer
	k_r=5.435×10^{-5} s^{-1}	
$fbn+TPA^f \rightleftharpoons TPA^b$	K_d=0.58 μmol/L	Husain et al[52]
	k_f=0.95833×10^{-4} μmol·L^{-1}·s^{-1}	1.5 sites/monomer
	k_r=6.658×10^{-5}·s^{-1}	
Reaction		
$plg^f+TPA^f \rightarrow plm^f$	In plasma	Hoylaerts et al[12]
	k_2=0.3 s^{-1}	
	K_m=28 μmol/L	
$plg^b+TPA^b \rightleftharpoons plm^b$	On fibrin	Zamarron et al[53]
	k_2=15.0 s^{-1}	
	K_m=0.13 μmol/L	
$plg^f+uPA \rightarrow plm^f$	Two-chain urokinase	Collen et al[54]
	k_2=1.0 s^{-1}	
	K_m=50.0 μmol/L	
$fbn+plm^b \rightarrow FDP$	k_{cat}=5 s^{-1}	Lottenberg et al,[55] Wu and Diamond[56]
$plm^f+AP \rightarrow [plm-AP]$	k''=10 μmol·L^{-1}·s^{-1}	Wiman and Collen[57]
$plm^f+MG \rightarrow [plm-MG]$	k''=0.3 μmol·L^{-1}·s^{-1}	Virca and Travis[58]
$TPA^f+PAI \rightarrow [TPA-PAI]$	k''=29 μmol·L^{-1}·s^{-1}	Lijnen et al[59]
$uPA^f+PAI \rightarrow [uPA-PAI]$	k''=20 μmol·L^{-1}·s^{-1}	Lijnen et al[59]
$plg^f+AP \rightleftharpoons [plg-AP]$	K_d=4.0 μmol/L	Wiman et al[60]
	k_f=1.087×10^{-4} μmol·L^{-1}·s^{-1}	
	k_r=4.348×10^{-4}·s^{-1}	

Additional abbreviations: plg indicates plasminogen; plm, plasmin; fbn, fibrin; MG, macroglobulin; f, free; and b, bound.

TPA levels during therapy was quite accurate because TPA levels were controlled simply through dilution of the bolus into the plasma and through its half-life, both of which are well characterized. These simulations demonstrated accurate prediction of systemic TPA levels (Fig 3), which can peak at >0.1 μmol/L after a bolus infusion of 50 mg.[13] Similarly, a double TPA bolus regimen of 35 mg in each bolus[20] was simulated with suitable accuracy. Simulation of the dynamic plasminogen level in the systemic circulation involved more biochemical interactions and required a suitable rate equation for plasminogen activation levels by TPA in plasma. The simulation provided agreement within ≈10% of measured plasminogen values (Fig 4) during lytic therapy for various clinical trials.[11,21-23] These trials involved the use of varying administrative schemes, from very modest to more aggressive TPA dosing. The prevailing α_2-antiplasmin and α_2-macroglobulin as well as free and inhibited plasmin levels are expected to be accurately predicted since they result directly from the prevailing plasminogen levels.

Predicting In Vitro Plasma Clot Lysis Under Conditions of Permeation

The next step was to validate predictions of clot lysis under various transport conditions created in vitro. We have previously shown[5] accurate simulation of plasmin-, uPA-, and TPA-mediated fibrinolysis under conditions of diffusional penetration of fibrinolytic mediators into purified fibrin gels (3 mg/mL) when the concentrations of these agents were physiological or within the clinical range (<1 μmol/L). For permeation velocities up to 1 mm/min, we have also accurately simulated the measured lysis front velocity of dissolving fibrin gels in vitro. In the present work, to recreate a transport regimen comparable to the convection-dominated nature of arterial thrombolytic therapy, a syringe pump was used to infuse a fibrinolytic mixture into PPP clots via permeation at a constant superficial velocity. Despite the apparent simplicity of this experimental configuration, a challenging test was to simulate the lysis of a PPP clot under the conditions of permeation given the numerous reactions that occur. A cocktail of 0.1 μmol/L TPA and 1.0 μmol/L Glu-plasminogen was placed adjacent to 2-cm-long PPP clots, and the superficial permeation velocity through the clot was maintained constant at 0.1 or 0.2 mm/min.

To simulate this experiment, the initial levels of the various fibrinolytic mediators in the clot were taken to be at values that were 66% of nominal values in plasma (Table 2) due to a one-third dilution during recalcification. Thus, the concentration of the fibrin was set initially as 5.823 μmol/L, and the fiber radius was set to 250 nm, resulting in an initial clot porosity of 0.9928. The initial total amount of AP in the clot was set at 0.66 μmol/L, and 30% of this value was treated as cross-linked to the fibrin phase (c_{AP}=0.4653 μmol/L, s_{AP}=27.719 μmol/L). The α_2-macroglobulin level was set at 2 μmol/L in the clot, all of which was in the fluid phase. A total concentration of 1.452 μmol/L plasminogen in the clot was allowed to equilibrate to the fibrin (K_d=38 μmol/L[24]), resulting in free and bound concentrations (c_{plg}=1.1094 μmol/L, s_{plg}=47.618 μmol/L) of plasminogen. Under these conditions, the simulation captured the measured rate of movement of the lytic front accurately (Fig 5). For prevailing inlet conditions of TPA (0.1 μmol/L), the bio-

TABLE 2. Initial State of Systemic Circulation and Arterial and Venous Thrombi

			Thrombi Level, μmol/L†	
	Plasma, μmol/L	α-Granule Release, μmol/L*	Venous	Arterial
Fibrin(ogen)	8.0	0.044	c_T=80–220	
Plasminogen†	2.2	0.00136	c_i=0.562	c_i=0.839
			s_i=1.299	s_i=2.428
			c_T=0.783	c_T=1.316
TPA†	0.00005	...	c_i=0.000618	c_i=0.000917
			s_i=0.00133	si=0.00309
			c_T=0.000832	c_T=0.00157
uPA	0.00005	...	c_i=0.00005	c_i=0.00005
			s_i=0	s_i=0
			c_T=0.000035	c_T=0.000035
Plasmin	0	...	...	...
PAI-1 (only 5% active)	0.0003	0.00447	c_i=0.0274	c_i=0.0617
			s_i=0.0071	s_i=0.00858
			c_T=0.0213	c_T=0.0458
AP‡	1.0	0.000269	c_i=1.0	c_i=1.0
			s_i=1.0	s_i=1.0
			c_T=1.0	c_T=1.0
Macroglobulin§	3.0	0.00171	c_i=3.0	c_i=3.0
			s_i=0	s_i=0
			c_T=2.1	c_T=2.1
Platelets‖	0.3×10^9/mL	...	1.5×10^9/mL‖	4.5×10^9/mL

*Based on release of α-granules from 0.3×10^9 platelets into 1 mL of buffer.

†Derived from Potter van Loon et al.[26] The pelleted wet weight, measured to be 30% of the thrombi weight, was assumed to be pure fibrin fibers. The overall density of the thrombi was assumed to be 1 g/mL. The published values (given in μg/g of thrombi of free and unbound species) were converted to local phase concentrations within the fluid (c_i) or within the fibrin (s_i). The free phase concentration c_i was calculated as (μg of free species/g of thrombi)·(g of thrombi/0.7 mL of fluid volume). For published values of bound species obtained from urea extracts of thrice-extracted, washed thrombi pellets, the bound species concentration s_i was calculated as (μg of bound species/g of thrombi)·(g of thrombi/0.3 mL of solid fibrin volume). For ϵ=0.7 corresponding to 0.3 g of pellet/g of thrombi, the total clot concentration of each species (c_T, μmol/L) is given as: $c_T=\epsilon\, c_i+(1-\epsilon)\, s_i$=(μg of free protein *i*/g of thrombi+μg of bound protein *i*/g of thrombi](1000/MW_i). MW_i indicates molecular weight of *i*th protein.

‡Assumed total concentration of 1 μmol/L antiplasmin present, of which 30% is cross-linked to fibrin.

§Assumed total concentration of 3.0 μmol/L macroglobulin present in the fluid phase of the clot.

‖Determined from thrombi PAI-1 antigen levels that were assumed to be derived entirely from platelets.

chemical reactions were occurring quite rapidly; however, the species transport (greatly enhanced through permeation relative to pure diffusion) remained rate limiting. This was seen where a doubling of the permeation velocity enhanced the lysis rate. The lysis front position in the experiment actually moved slightly ahead of the position of the perfusion front ($\bar{v}t$) because of dispersion processes that were captured in the simulation with Equation 7. In contrast to the permeation results shown in Fig 4, the lysis front proceeded only 1.1 mm in 60 minutes through diffusional transport ($\bar{v}$=0) of TPA and plasminogen into a PPP clot. Thus, permeation at a velocity of 0.2 mm/min caused a 15-fold increase in the lysis rate compared with diffusional delivery.

In addition to determination of lysis front position with time, the concentration profiles of the species were simulated at all times corresponding to the experiments shown in Fig 5. At 30 minutes after the initiation of permeation at 0.2 mm/min, the front moved ≈8 mm as indicated by the data point with an asterisk in Fig 5. For the simulation of this experiment at 30 minutes, the free-phase profiles are shown for plasminogen, plasmin, and TPA (Fig 6A). Robust lysis was predicted to occur in the region of the lysis front where TPA was present at low but catalytic levels. The level of plasmin in the free phase was very small due to rapid inhibition by the free-phase antiplasmin and macroglobulin as well as by the cross-linked antiplasmin that was liberated during lysis into the fluid phase. Due to solubilization of bound (nonactivated) plasminogen over the preceding 30 minutes of the simulation, there was a small peak in the plasminogen concentration near the front. In Fig 6B, the bound phase concentrations based on the total volume of the clot, $s_i\cdot(1-\epsilon)$, are shown. Behind the lysis front, the bound concentrations of species in the fibers s_i were the residual levels of species left in vanishingly thin fibers. These concentrations reached very high values but occur in zones of >99.99% lysis and represent negligible amounts of species because $s_i\cdot(1-\epsilon)\approx0$ in these regions. The bound levels of the various proteins displayed a maximum at the lysis front, which was a thin zone where significant plasminogen activation and lysis were occurring. The local rate of lysis was reduced by the clot levels of the fast-acting plasmin inhibitors. These inhibitors and complexes are shown in Fig 6C. In the zone of full lysis behind the front, the inhibitors were depleted through complexation and perfusion of inhibitor-free liquid (a washout effect since only TPA and plasminogen were perfused into the clot). At the lysis front, the concentration of plasmin/antiplasmin was substantially higher than that of plasmin/macroglobulin because of the faster inhibition rate of antiplasmin. The slight peak in free antiplasmin levels was due to release of fibrin-bound antiplasmin during lysis at the advancing front over the preceding 30 minutes. Overall, these simulations indicate that substantial lysis had occurred in the regions where TPA had penetrated to even a small extent. Also, the rate of lysis front advancement was controlled by the rate of permeation of the fibrinolytic mediators.

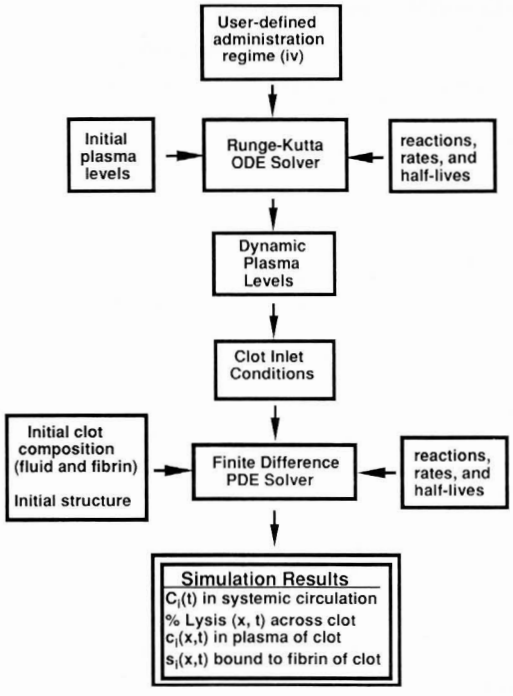

FIG 2. Numerical algorithm for predicting systemic and clot lysis dynamics for intravenous thrombolytic therapy.

Prediction of Arterial Thrombi Dissolution by Intravenous TPA or uPA Therapy

The superficial velocity of permeation through a clot is dictated by the pressure drop across the thrombus and

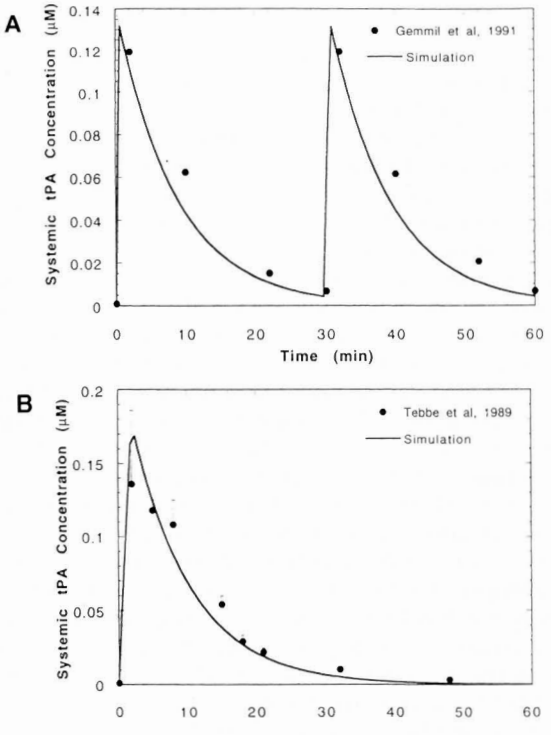

FIG 3. Comparison of simulated circulating levels of TPA (solid lines) with data (solid circles) obtained from clinical trials for various administration regimens. For TPA administration, measured plasma levels of TPA are shown as a function of time for a double 35-mg bolus[20] (A) and a 50-mg bolus[21] (B).

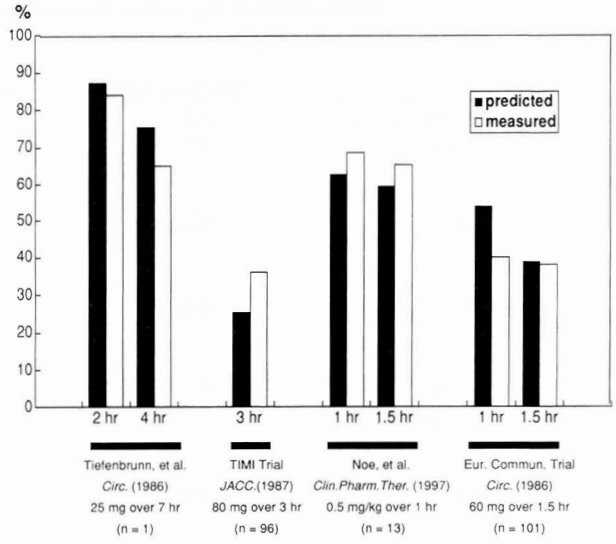

FIG 4. Prediction of systemic circulating levels of plasminogen for four separate TPA administration regimens. The plasminogen levels are predicted and compared with measured values.[11,21-23]

the specific permeability of the clot. Over the cardiac cycle, the time-averaged permeation velocity depends on the time-averaged pressures both proximal and distal to the clot. The upstream pressure is the time-averaged aortic pressure of ≈90 mm Hg, whereas the downstream pressure depends on the extent of collateralization. In the absence of collateralization, the time-averaged downstream pressure may be only slightly higher than the mean right atrium pressure of ≈10 to 20 mm Hg. With collateralization, higher mean pressures of 40 to 50 mm Hg may occur distal to the clot and may provide delivery of the agent to the distal face of the clot (not considered in the present study). For a 1-cm-long clot, the pressure drop across an occlusive arterial thrombus may range from ≈50 to 80 mm Hg/cm (without collateralization) to ≈40 mm Hg/cm with collateralization. During MI, the precise phasing of the pulsatile aortic pressure with the pressures distal to the occluding thrombus in a blocked coronary artery is not well defined at present. Over the

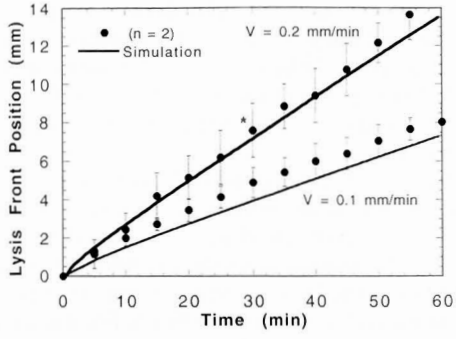

FIG 5. Simulation and measurement of TPA-mediated lysis of PPP clots (n=2) under conditions of constant superficial permeation velocity as a lysis front moves across the 2-cm-long clot. A mixture of TPA (0.1 μmol/L) and Glu-plasminogen (1 μmol/L) was perfused at constant permeation velocities of 0.1 and 0.2 mm/min into plasma clots (formed at 33% dilution after recalcification). Simulation results (solid lines) and measured front position (solid circles) are shown versus time. The simulated concentration profiles within the dissolving clot at 30 minutes for the clot dissolved by infusion at 0.2 mm/min (*) are given in Fig 6.

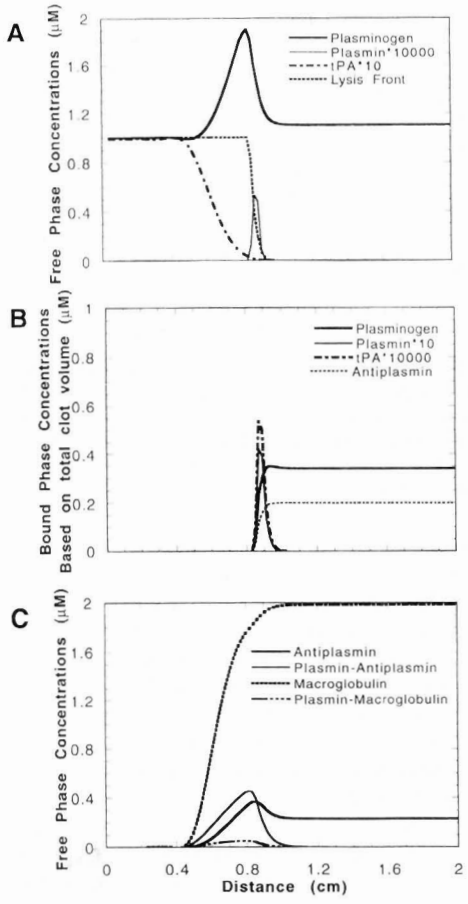

FIG 6. Simulation of spatial concentrations after 30 minutes when TPA (0.1 μmol/L) and plasminogen (1.0 μmol/L) were perfused into PPP clots at a constant superficial velocity of 0.2 mm/min. The lysis front has moved to a position of ≈1 cm into the clot after 30 minutes of lysis. Note that some concentrations are multiplied by a factor of 10 or 10 000 to facilitate presentation. The lysis front profile (A) can be multiplied by 100 to give percent lysis.

cardiac cycle, the clot will essentially time-average the pulsatile flow, whereas dispersive processes are likely enhanced by the pulsatility.[25]

Thrombi have structures and compositions that are dependent on their age and the prevailing hemodynamic conditions during their formation. The biochemical compositions of venous and arterial thrombi have been measured ex vivo,[26] and these values are given in Table 2, recalculated for the fluid and fibrin phases. There are very few direct measurements of the amount of fibrin within human thrombi. In Table 2, we took as a worst case scenario that the entire mass of insoluble material of urea-extracted and thrice-washed thrombi measured by Potter vann Loon et al[26] is hydrated fibrin (this neglects the wet weight of insoluble platelet actin and cell debris). See "Appendix 3" for details.

Using in vitro kinetic data (Table 1) for the reaction network (Fig 1) and ex vivo arterial thrombi properties and initial plasma composition (Table 2), we simulated a prototype accelerated therapeutic regimen for intravenous TPA therapy for coronary thrombolysis[27] involving a 15-mg bolus followed by infusion of 85 mg over 90 minutes. In the simulation, this regimen provided for a relatively constant circulating level of TPA of ≈0.04 μmol/L (Fig 7A) during the first hour of therapy. Plasminogen dropped to less than half of its original level with concomitant consumption of antiplasmin and macroglobulin and appearance of plasmin/antiplasmin and plasmin/macroglobulin complexes in the circulation by 1 hour.

The lysis front advanced at a nearly constant velocity of ≈1 mm every 10 minutes for the first 40 minutes of the therapy (Fig 7B), after which lysis proceeded more rapidly with the remaining 6 mm of the thrombi dissolving in the next 10 minutes. This acceleration toward reperfusion that occurred between 40 and 50 minutes after initiation of the therapy was due to the shortening of the clot at constant proximal pressure head (increasing pressure drop and permeation) and accumulation of reaction species at the lysis front. The prediction of clot lysis (with no adjustable parameters) is consistent with observed recanalization times between 45 and 90 minutes.

To indicate the reaction dynamics during the simulation, "snapshots" of the initial 1-cm clot domain after 10 minutes of therapy are shown in Fig 7C through 7E. At 10 minutes, the lysis front advanced over 1.2 mm into the clot, and the most active lysis zone was seen to be a region of ≈0.25-mm thickness. In this thin reaction zone, dramatic changes in reactant concentrations were seen. Some fibrin-bound plasminogen was released through solubilization, and this plasminogen readsorbed and accumulated at the lysis front to levels in excess of prevailing plasma levels. Under conditions of permeation for 10 minutes in the simulation, the continual binding of TPA at the lysis front resulted in TPA levels that were twofold to threefold higher than circulating levels. Interestingly, antiplasmin and macroglobulin were predicted to become depleted in the "spent" fluid that was moving with the lysis front (Fig 7E), allowing plasmin to exist as a long-lived species. This was because the reacting fluid at the lysis front was continually reaching plasminogen-laden fibrin that was activated (Fig 7E) and lysed with the released plasmin subsequently inhibited. The free plasmin predicted to exist in the antiplasmin- and macroglobulin-depleted zone would be susceptible to the slower C1 inhibitor (not simulated). We predict that some plasmin/C1 inhibitor complex would form under permeation conditions despite the known kinetic disadvantage of C1 inhibitor in well-mixed systems. The inhibited plasmin complexes formed at the lysis front had no fibrin binding capability (Fig 1) and thus moved with the permeating fluid. This was seen in Fig 7E, where the inhibited complexes penetrated ≈1 mm farther ahead of the lysis front after 10 minutes of lysis. The lysis front was moving at a velocity slower than the permeation velocity but much faster than would be expected in the absence of pressure-driven permeation. We conclude that in Fig 7, the overall thrombolytic rate (ie, lysis front velocity) achieved as a result of the dosing scheme for this clot structure and composition can be improved only up to the point where the lysis front proceeds at a velocity comparable to the permeation velocity. Once this maximal lysis rate is achieved with higher dosing, further increases in TPA dosage or dosage rate would not offer significant gain. In contrast to Fig 7, the more robust fibrinolysis achieved in the in vitro experiment (Figs 5 and 6) resulted in a lysis front with a velocity that was comparable to the permeation front velocity.

The prevailing systemic levels of circulating species at 10 minutes (see Fig 7A) exist at the inlet of the initial reaction domain at x=0 cm (Fig 7C and 7E). In a one-dimensional

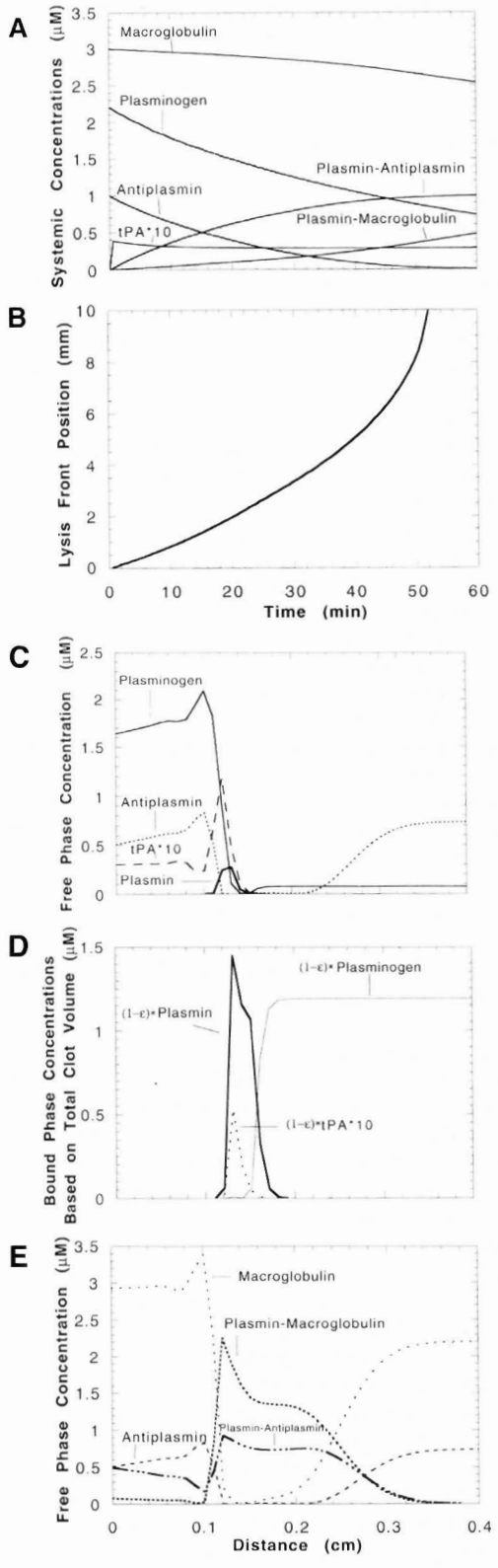

FIG 7. Lysis of an arterial thrombus by intravenous TPA thrombolytic therapy (100 mg total dose). Changes in systemic species are shown (A) for a therapy initiated by a 15-mg TPA bolus followed by infusion of 85 mg TPA over 90 minutes. Initial clot length is 1 cm, and initial pressure drop was set at 50 mm Hg/cm. Complete reperfusion is achieved at 52 minutes (B). The lysis and concentration profiles of free and bound species (C through E) across the clot are shown after 10 minutes of therapy.

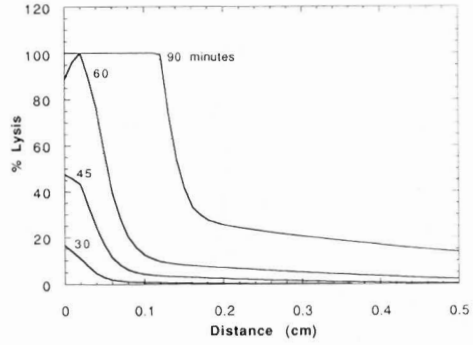

FIG 8. Fibrinolysis of an arterial thrombus mediated by two-chain uPA under conditions of intravenous thrombolytic therapy. The percent lysis profiles across a 1-cm arterial thrombus are shown at various times for a therapy consisting of 8-mg bolus followed by infusion at 1 mg/h. Initial pressure drop, clot structure, and clot composition are the same as in Fig 7.

simulation, mixing eddies proximal to the clot cannot be simulated since the reacting fluid can move only in the forward direction. Thus, changes in systemic concentrations were not immediately and directly having an impact on reaction dynamics at the lysis front. Rather, changes in the systemic concentrations of species were immediately manifest at the inlet of the initial reaction domain and then began to convect forward. In this one-dimensional approach, the biochemistry of the plasma that reaches the proximal face of the clot in the first minutes of the therapy had the greatest impact on subsequent dynamics. This is consistent with the motivation for front-loaded therapies.[28] In the simulation, the permeation of fluid through the lysis front was somewhat faster than the movement of the lysis front, and the constituents of this fresh plasma fed the reactions at the lysis front to a significant extent during the first 10 minutes of the therapy but less so thereafter. (See "Discussion" regarding inlet mixing.)

To demonstrate the marked qualitative and quantitative differences between uPA and TPA, we conducted a simulation of intravenous urokinase (two-chain uPA) therapy for acute MI. At the present, we have not included in the kinetic model the conversion by plasmin of single-chain uPA (pro-urokinase) to the active two-chain uPA. We used a protocol of a bolus of 8 mg uPA ($\approx 10^6$ IU Abbokinase) followed by a continuous infusion of 1 mg/h ($\approx$125 000 IU/h), which provided for an approximately constant level of 0.04 μmol/L uPA in the systemic plasma. In the simulation, since uPA is active in the plasma, a rapid and nearly complete activation of circulating plasminogen was observed within 1 hour after initiation of the therapy, with consequent consumption of antiplasmin and macroglobulin. In contrast to TPA, after 30 minutes of intravenous uPA infusion, only a minor amount of lysis took place (Fig 8). With uPA, the marked depletion of systemic plasminogen in combination with generation of plasmin in the free phase, where it was rapidly inhibited, resulted in rather inefficient therapy compared with TPA. By 90 minutes, antiplasmin was predicted to become depleted in the front of the clot due to washout with the antiplasmin free circulating plasma and continual activation of plasminogen released from the dissolving fibrin (simulation not shown). A zone of complete lysis proceeded $\approx$1.5 mm across the front of the clot at 90 minutes. Also, lesser degrees of lysis (5% to 30%) were present at 90 minutes in regions deep within the clot (0.2 to 1 cm). This deep zone of lysis was not seen with TPA and indicates that uPA activated an inner clot pool of plasminogen because its penetration into the clot was

not slowed by binding. The distinct patterns of TPA and uPA thrombolysis make the deconvolution of additive versus synergistic biochemical effects of combined TPA/uPA intravenous therapies difficult, since low levels of uPA-mediated inner clot lysis may enhance permeation of TPA (a likely beneficial effect that is based in transport).

Discussion

We developed a computer algorithm to relate the dynamics of the systemic circulation to the thrombolytic processes that occur at the site of a dissolving thrombus during thrombolytic therapy. The model made accurate predictions of circulating TPA and plasminogen levels measured during clinical trials for intravenous TPA therapy. Also, the model made accurate predictions of in vitro plasma clot lysis under conditions of permeation. Finally, arterial thrombolysis was simulated for TPA and uPA intravenous administration. The simulations provided rates of overall lysis as well as spatial distributions of reacting species.

As a one-dimensional model, the simulations describe the rate at which a lysis front proceeds across a given clot structure. In these one-dimensional simulations, fluid can advance only in the forward direction. Thus, the simulation cannot be used to describe radial fluxes within a clot, dissolution fingering,[2,29,30] or fluid mixing at the proximal face of the clot. A common approach to account for eddy mixing at the inlet of a reaction domain is to increase the longitudinal dispersion coefficient, D_L. We implemented this approach by increasing D_L by 20-fold at all positions of the clot that were 100% lysed. This led to modest increases ($\approx$20% to 30% at 15 minutes) in the rate of lysis. Still, this approach does not fully capture the impact of mixing at the proximal face of the dissolving clot. The one-dimensional model used in the present study would correspond to anatomic situations where the thrombi are a substantial distance from a well-mixed region that exists upstream at a vessel bifurcation. If coagulated red blood cells accumulate on the proximal face of the clot due to thrombin leakage, blood stagnation, and/or plasma infiltration into the thrombus, this loose structure would offer little resistance to permeation but would damp fluid mixing proximal to the clot. The hemodynamics of this situation are captured in one-dimensional simulations.

A two- or three-dimensional model is required to predict the causes and probability of lytic fingering where dissolution channels proceed through the clot to produce early but low-grade reperfusion. When a channel begins to develop, its growth is fortified by the development of larger pressure gradients at the leading tip of the finger, with consequent faster permeation and accumulation of binding species. Using a two-dimensional model,[30] we found that large lytic fingers will occur when the initial thrombus contains a spatial distribution of random fluctuations in initial fibrin density as small as $\pm$10% (on average).

Thrombolysis occurs in the presence of continued coagulation. New fibrin deposition by thrombin released or generated in the clot can be taken into account by allowing the porosity at a particular clot location ($\partial\epsilon/\partial t$ in Equation 2) to be a function of both lysis and coagulation. In such a model, continuing coagulation within a dissolving thrombus would likely dictate a threshold level of plasminogen activator needed to achieve net lysis as well as indicate some benefit to local clot lysis by systemic fibrinogen consumption.

Less is known quantitatively about the range of permeation flows through real human arterial thrombi during MI. The permeation of plasma through a clot may be nonuniform and slow compared with nominal flow rates through the coronary vessels. Superficial permeation velocities across coronary thrombi are estimated to be $\leq\approx$0.001 cm/s.[4,5] To obtain reperfusion within 45 to 90 minutes, some permeation of the lytic agent into the clot must occur since diffusion is such a slow transport process.[1-5,10] As Blinc et al[31] pointed out, permeation must occur when radiolabeled fibrinogen injected into dogs with existing occlusive coronary clots is found to be distributed along the clot length in $<$1 hour.[32] Diffusional transport would require days or weeks to achieve this distribution.

Clinical evidence also indicates an important role for permeation and its impact on the rate at which reperfusion occurs. The role of permeation is apparent in the observation that patients with hypotension or cardiogenic shock are poor candidates for successful thrombolytic treatment of MI.[6,33] The impact of pressure-driven permeation of lytic agents into clot structures was demonstrated in a canine model of LAD thrombosis under conditions of severe hypotension (systolic pressure of 75 mm Hg).[7] A LAD catheter administration of TPA to the clot was significantly less effective under conditions of hypotension compared with thrombolysis at systolic pressures of 130 mm Hg.[7] Under either condition of 75 and 130 mm Hg systolic blood pressure, the delivery of the agent to the proximal face of the clot was the same (by intracoronary catheter); however, the driving pressures for permeation were markedly different. Similar transport mechanisms have been shown for the lysis of pulmonary embolism.[34,35] In human cardiogenic shock and MI, the success of thrombolytic therapy can be enhanced with the administration of inotropic agents (with consequent increase of systolic pressure from 64 to 102 mm Hg).[6] In a canine model of cardiogenic shock with LAD thrombosis in which systolic blood pressure had been reduced to 75 mm Hg through phlebotomy, intra-aortic balloon counterpulsation to increase coronary pressure resulted in enhanced thrombolysis with the use of intravenous TPA.[8,36]

Studies with ultrasound also demonstrate the importance of transport processes. Francis et al[37] demonstrated that 1-MHz ultrasound at intensities of $\leq$8 W/cm^2 significantly enhanced the rate of lysis of a plasma clot submerged in solutions of TPA (1 μg/mL) as well as uPA. Such levels of ultrasound do not cause fragmentation or heating of the thrombus; rather, micromixing and transport facilitation are the causes of enhanced lysis. Through a cavitation-dependent mechanism, ultrasound was shown to facilitate transport of reactants without modulation of enzymatic activity.[38] When ultrasound is applied to fibrin clots that are maintained under a hydrostatic pressure head, the permeability also increases through a cavitation-dependent mechanism that alters fibrin fiber structure.[39] Enhancement in permeability through ultrasound facilitated pressure-driven permeation of lytic agents into the whole blood clot with consequent reduction of reperfusion times.[40]

Specific structural aspects of clots have received attention with respect to lytic susceptibility and penetration of lytic agents. For example, coronary artery thrombi formed during unstable angina tend to be grayish white, whereas those present during acute MI are reddish, as determined with angioscopy.[41] These grayish-white coronary thrombi

tend to be resistant to thrombolytic therapy.[42] These structures are particularly rich in platelets, are older, and have a very tight fibrin structure,[43] and they are believed to be formed under flow conditions. The reddish thrombi of acute MI are rich in fibrin and red blood cells and tend to be younger and formed under conditions of stasis. It is certainly possible that the tight fibrin (possibly also containing collagen) networks of aged thrombi do not allow sufficient penetration of lytic agents.

The transport limits are difficult to overcome; it is difficult for a plasminogen activator to penetrate the many centimeters into the long clots of the deep veins or peripheral arteries. Pressure drops across the long venous clots are likely to be an order of magnitude less than the pressure drops across arterial thrombi. Aggressive systemic intravenous therapies are not typically used in these instances. For these clots, catheters are introduced either directly into the clot[44] or with guide wires to help open a channel in the thrombus for perfusion.[45,46]

With the advent of new delivery schemes, administration regimens, and agents, computer simulation is an additional tool for the streamlined evaluation of new therapies. Knowledge of the theoretical optimality of a given approach provides a benchmark by which to evaluate the efficacy of the administration regimen and agent. The methods described in the present work also facilitate an understanding of the dynamics and evaluation of the efficacy of intravessel or intrathrombic delivery of thrombolytic agents.

Appendix 1: Theory

To quantify the change in fibrin fiber volume on lysis, the total length of fibers initially in the gel was first evaluated (for uniform initial radius R_{fo}). The total length of fibers is related to the fibrin fiber density (ρ_{fiber}), the gel density (ρ), and the total clot volume, V_T (cm^3). The total length of fibers per volume of gel is given as[4]

$$\frac{L_T}{V_T}=\frac{\rho_0 \cdot 10^{21} nm^3/cm^3}{\rho_{fiber}(\pi R_{fo}^2)} \quad (10)$$

for L_T and R_{fo} [=] nm.

The local dynamic change in fibrin gel porosity (ϵ) was related to the local extent of lysis (L) by allowing the radius of the fibers (R_f) to shrink at constant fibrin fiber density (ρ_{fiber}= 0.28 g/mL of fiber[47] and $s_o=\rho_{fiber}/M_W$ monomer), whereas the fiber length per unit volume of gel (L_T/V_T) was assumed to remain constant (Equations 10 and 11).

$$R_f(x,t)^2=(R_{fo}^2)\cdot\frac{s_o-L(x,t)}{s_o} \quad (11)$$

For an initial fiber radius (R_{fo}) and a total fiber length density, L_T/V_T, the initial gel porosity is

$$\epsilon_o=1-\pi R_{fo}^2(L_T/V_T)10^{-21}cm^3/nm^3=1-(\rho_o/\rho_{fiber}) \quad (12)$$

The local instantaneous porosity $\epsilon(x,t)$ based on the local instantaneous fiber radius, $R_f(x,t)$, is calculated similarly. The percent lysis is then known at any position by

$$\%\ \text{Lysis}(x,t)=\left[1-\left(\frac{R_f(x,t)}{R_{fo}}\right)^2\right]\cdot 100=\frac{L(x,t)}{S_o}\cdot 100 \quad (13)$$

The local concentration of each type of binding site (θ_r) within the fiber is determined by the fibrin monomer concentration within the fiber (s_o, assumed constant during lysis as the fiber radius shrinks) multiplied by the sites per monomer, q_r. We have kept q_r constant in the present work. The local specific permeability $k(x,t)$ is calculated from $\epsilon(x,t)$ and $R_f(x,t)$ with Equation 8. At any given time, t′, the overall specific permeability $\bar{k}$ can be evaluated as the inverse of the total resistivity by integrating the local resistivity $[k(x,t')]^{-1}$ over the length of the clot for a one-dimensional system.

Appendix 2: Numerical Methods

The concentration (C_i) of each species in the systemic circulation was obtained through solution of the system of coupled ordinary differential equations (Equation 1) describing the plasma as a one-compartment system with time-dependent sources (intravenous infusion) and sinks (liver clearance). The integration of the equations was accomplished with a fourth-order Runge-Kutta solver.[48] To simulate realistic infusion regimens of any fibrinolytic mediator, the Runge-Kutta solver was designed so that bolus (mg) or continuous infusions (mg/min) could be specified directly for any infusion regimen, I(t). Prevailing systemic concentrations were based on the plasma volume of 3.5 L. Bolus infusions were treated as rapid continuous infusions that occur over a 5-second interval. The concentrations of the species in the systemic circulation were calculated for every 1 millisecond of simulation and served as inlet conditions (C_i^{inlet}) for the Danckwerts boundary conditions (Equation 5) for each species balance partial differential equation.

A finite difference algorithm was used to solve the system of coupled and nonlinear PDEs. A two-step procedure was used to advance the solution from the j to the $j+1$ time level via a differencing formulation at the $j+1/2$ time level as previously described.[5] During lysis, the transport and material properties (D_{fiber}, D_L, k, ϵ, $\bar{v}$) within the clot change in time and space. To begin, the values are known at every node in the domain at the j time level for the free and bound concentrations of each species (c_i, s_i), the fiber radius, porosity, and percent lysis. The use of a specialized algorithm for improved material property guesses at the $j+1/2$ level for the porosity and fiber radius provided for a straight forward solution of c^{j+1}. On calculation of the transport properties at the $j+1/2$ and $j+1$ levels, the free-phase concentrations at the $j+1$ time level can be obtained through gaussian elimination of finite difference matrices evaluated at the $j+1/2$ level. We observed a monotonic rate of convergence (1 to 25 iterations). For simulations with numerous fast reacting and convecting species through erodible fibrin, a simulation of 60 minutes of lysis required <8 hours of CPU (Silicon Graphics Indigo R4000 or SUN SparcCenter 2000) using $\Delta t=0.01$ second and 0.01-cm node spacing. The conservation of mass of each species for the total system (both free and bound phases) has been rigidly implemented to ≤0.5%.

Appendix 3: Clot Composition and Permeability

The total volume of a thrombus can be subdivided into the volume occupied by cells and the volume occupied by the biphasic fibrin gel (hydrated fibrin fiber volume plus water volume). The model (Equations 2 through 9) describes phenomena in the biphasic fibrin gel that exists between the cells. Since the thrombus forms under flow conditions, the relationship of clot properties to those of whole blood is not a direct one because depletions and enrichments occur. During thrombosis under flow, platelets accumulate in the growing clot to levels that are 5 to 15 times higher than the plasma concentration (of 300 000/μL). This conclusion is based on measurements of PAI-1 levels in thrombi[26,49] where PAI-1 levels are 200 times plasma levels and ≈5 to 15 times higher than serum levels (containing platelet PAI-1 released from α-granules). Also, the volume occupied by red blood cells within the thrombus volume is very likely to be lower than blood hematocrit. This conclusion is based on (1) the existence of white and pink thrombi that occur under arterial conditions and (2) the low red blood cell content of thrombi formed under high flow in vitro. In a thrombus, the concentration of fibrin in the volume occupied by the biphasic fibrin gel is expected to

greatly exceed its plasma level (8 μmol/L) and likely has a concentration ranging from 80 to $\approx$220 μmol/L. This conclusion is based on in vitro and ex vivo studies. Coagulated platelet-rich plasma can retract to $\approx$10% of its original volume, resulting in a 10-fold enrichment of the resulting thrombus concentration of fibrin. Clotted whole blood can retract to $\approx$50% of its original volume. Since the original red blood cell volume within the retracted whole blood clot is unchanged during retraction, the fibrin gel volume has lost considerable serum and in effect has been condensed to only $\approx$10% of its original volume, resulting in a high fibrin concentration ($\approx$80 μmol/L) in the gel space of the thrombus. During its formation, a real thrombus is subjected to hemodynamic forces that may further consolidate the fibrin gel of the thrombus. Also, the permeation of fresh fibrinogen into the clot may allow continuing fibrin polymerization due to high levels of inner clot thrombin. Platelet release of fibrinogen (50 μg/10^9 platelets at $\approx 3\times10^9$/mL of thrombi) represents a relatively minor contribution to the fibrin content of a platelet-retracted thrombus (<1%). The estimate of the high density of fibrin (80 to 200 μmol/L) in a thrombus is consistent with direct measurements of the insoluble, washed wet pellet (wet fibrin fibers plus insoluble wet cellular debris), which represents 31% of the total thrombus weight obtained from arterial and venous thrombi.[26] This wet pellet likely contains substantial fibrin, based on the earlier report by Brommer et al[50] that fibrin represents 85% of the dry weight of fresh human arterial thrombi. The weight of pelleted wet fibrin fibers from an 80 μmol/L fibrin gel is calculated to be $\approx$10% of the original wet weight of the gel based on a fibrin fiber density of 280 mg of fibrin/mL of fiber[47] for fibers that are 80% water. Similarly, the weight of pelleted wet fibrin fibers from a 220 μmol/L fibrin gel is calculated to be $\approx$27% of the original wet weight of the gel.

Acknowledgments

This work was supported by an American Heart Association, National Center, grant (93-8670) and by National Science Foundation grant BES 9358236. Also, we acknowledge the SUNY School of Engineering and Applied Sciences for use of the SUN SparcCenter 2000 machine as well as National Science Foundation Instrumentation Grant CTS 9212682 to Dr T.J. Mountziaris for use of the SGI R4000 machine.

References

1. Blinc A, Planinsic G, Keber D, Jarh O, Lahajnar G, Zidansek A, Demsar F. Dependence of blood clot lysis on the mode of transport of urokinase into the clot: a magnetic resonance imaging study in vitro. *Thromb Haemost*. 1991;65:549-552.
2. Blinc A, Keber D, Lahajnar G, Stegnar M, Zidansek A, Demsar F. Lysing patterns of retracted blood clots with diffusion or bulk flow transport of plasma with urokinase into clots: a magnetic resonance imaging study in vitro. *Thromb Haemost*. 1992;68:667-671.
3. Wu JH, Siddiqui K, Diamond SL. Transport phenomena and clot dissolution therapy: an experimental investigation of diffusion-controlled and permeation-enhanced fibrinolysis. *Thromb Haemost*. 1994;72:105-112.
4. Diamond SL, Anand S. Inner clot diffusion and permeation during fibrinolysis. *Biophys J*. 1993;65:2622-2643.
5. Anand S, Wu JH, Diamond SL. Enzyme-mediated proteolysis of fibrous biopolymers: dissolution front movement in fibrin and collagen under conditions of diffusive and convective transport. *Biotech Bioeng*. 1995;48:89-107.
6. Garber PJ, Mathieson AL, Ducas J, Patton JN, Geddes JS, Prewitt RM. Thrombolytic therapy in cardiogenic shock: effect of increased aortic pressure and rapid tPA administration. *Can J Cardiol*. 1995; 11:30-36.
7. Prewitt RM, Gu S, Garber PJ, Ducas J. Marked systemic hypotension depresses coronary thrombolysis induced by intracoronary administration of recombinant tissue-type plasminogen activator. *J Am Coll Cardiol*. 1992;20:1626-1633.
8. Prewitt RM, Gu S, Schick U, Ducas J. Intraaortic balloon counterpulsation enhances coronary thrombolysis induced by intraveneous administration of a thrombolytic agent. *J Am Coll Cardiol*. 1994; 23:794-798.
9. Miller RD, Burchell HB, Edwards JE. Myocardial infarction with and without acute coronary occlusion: a pathological study. *Arch Intern Med*. 1951;88:597-611.
10. Zidansek A, Blinc A. The influence of transport parameters and enzyme kinetics of the fibrinolytic system thrombolysis: mathematical modeling of two idealized cases. *Thromb Haemost*. 1991; 65:553-559.
11. Tiefenbrunn AJ, Graor RA, Robison AK, Lucas FV, Hotchkiss A, Sobel BE. Pharmacodynamics of tissue plasminogen activator characterized by computer-assisted simulation. *Circulation*. 1986;73: 1291-1299.
12. Hoylaerts M, Rijken DC, Lijnen HR, Collen D. Kinetics of the activation of plasminogen by human tissue plasminogen activator. *J Biol Chem*. 1982;257:2912-2919.
13. Tebbe U, Tanswell P, Seifried E, Feuerer W, Scholz KH, Herrman KS. Single bolus injection of recombinant tissue-type plasminogen activator in acute myocardial infarction. *Am J Cardiol*. 1989;64: 448-453.
14. Kohler M, Sen S, Miyashita C, Hermes R, Pindur G, Heiden M, Berg G, Morsdorf S, Leipnitz, Zeppezauer M, Schieffer H, Wenzel E, Schonberger A, Hollemeyer K. Half-life of single chain urokinase-type plasminogen activator (scu-PA) and two-chain urokinase-type plasminogen activator (tcu-PA) in patients with acute myocardial infarction. *Thromb Res*. 1991;62:75-81.
15. Park IH, Johnson CS, Jones MR, Gabriel DA. Probes of fibrin gel porosity. In: Mosesson MW, Amrani DL, Siebenlist KR, DiOrio JP, eds. *Fibrinogen and Biochemistry: Biological Functions. Gene Regulation and Expression*. Amsterdam, Netherlands: Excerpta Medica; 1988:123-128.
16. Matveyev MY, Domogatsky SP. Penetration of macromolecules into contracted blood clots. *Biophys J*. 1992;63:862-863.
17. Sahimi M, Hughes BD, Scriven LE, Davis HT. Dispersion in flow through porous media: one-phase flow. *Chem Eng Sci*. 1986;41: 2103-2122.
18. Dullien FA. *Porous Media: Fluid Transport and Pore Structure*. New York, NY: Academic Press; 1979.
19. Ranby M, Brandstrom A. Control of t-PA mediated fibrinolysis. In: Kluft C, ed. *Tissue-Type Plasminogen Activator (t-PA)*. Boca Raton, Fla: CRC Press; 1988:211-224.
20. Gemmill JD, Hogg KJ, MacIntyre PD, Booth N, Rae AP, Dunn FG, Hillis WS. A pilot study of the efficacy and safety of bolus administration of alteplase in acute myocardial infarction. *Br Heart J*. 1991;66:134-138.
21. Mueller HS, Rao AK, Forman SA, and the TIMI Investigators. Thrombolysis in Myocardial Infarction (TIMI): comparative studies of coronary reperfusion and systemic fibrinolysis with two forms of recombinant tissue-type plasminogen activator. *J Am Coll Cardiol*. 1987;10:479-490.
22. Noe DA, Bell WR. A kinetic analysis of fibrinolysis during plasminogen activator therapy. *Clin Pharm Ther*. 1987;41:297-303.
23. Collen D, Bounameaux H, DeCock F, Lijnen HR, Verstraete M. Analysis of coagulation and fibrinolysis during intravenous infusion of recombinant human tissue-type plasminogen activator in patients with acute myocardial infarction. *Circulation*. 1986;73:511-518.
24. Lucas MA, Fretto LJ, McKee PA. The binding of human plasminogen to fibrin and fibrinogen. *J Biol Chem*. 1983;258:4249-4256.
25. Thurston GB, Henderson NM. Impedance of a fibrin clot in a cylindrical tube: relation to clot permeability and viscoelasticity. *Biorheology*. 1995;32:503-520.
26. Potter van Loon BJ, Rijken DC, Brommer EJP, van der Maas APC. The amount of plasminogen, tissue-type plasminogen activator, and plasminogen activator inhibitor type 1 in human thrombi and the relation to ex-vivo lysibility. *Thromb Haemost*. 1992;67:101-105.
27. Wall TC, Califf RM, George BS, Ellis SG, Samaha J, Kereiakes DJ, Worley SJ, Sigmon K, Topol EJ, for the TAMI-7 Study Group. Accelerated plasminogen activator dose regimens for coronary thrombolysis. *J Am Coll Cardiol*. 1992;19:482-489.
28. Levine MN. Bolus, front-loaded, and accelerated thrombolytic infusions for myocardial infarction and pulmonary embolism. *Chest*. 1991;99:128S-134S.
29. Zidansek A, Blinc A, Lahajnar G, Keber D, Blinc R. Finger-like lysing patterns of blood clots. *Biophys J*. 1995;69:803-809.
30. Anand S, Diamond SL. Simulations of systemic circulation dynamics and consequent thrombi dissolution rates during intravenous thrombolytic therapy. American Institute of Chemical Engineering 1995 Annual Meeting, November 13, 1995, 478. Abstract.
31. Blinc A, Kennedy SD, Bryant G, Marder VJ, Francis CW. Flow through clots determines the rate and pattern of fibrinolysis. *Thromb Haemost*. 1994;71:230-235.

32. Moschos CB, Oldewurtel HA, Haider B, Regan TJ. Effect of coronary thrombus age on fibrinogen uptake. *Circulation*. 1976;54: 653-656.
33. Prewitt RM. Thrombolytic therapy in patients where hypotension and cardiogenic shock complicate acute myocardial infarction. *Can J Cardiol*. 1993;9:155-157.
34. Prewitt RM, Gu SA, Greenberg D, Chan SM, Schick U, LaPointe H, Ducas J. Effects of flow on recombinant tissue plasminogen activator-induced pulmonary thrombolysis. *J Appl Physiol*. 1991; 71:1441-1446.
35. Prewitt RM, Downes AM, Gu SA, Chan SM, Ducas J. Effects of hydralazine and increased cardiac output on recombinant tissue plasminogen activator-induced thrombolysis in canine pulmonary embolism. *Chest*. 1991;99:708-714.
36. Prewitt RM, Gu S, Schick U, Wiens A, Ducas J. The effect of a moderate increase in a low coronary artery inflow pressure on coronary thrombolysis induced by intraveneous administration of recombinant tissue plasminogen activator. *Thromb Haemost*. 1993;69: 1353. Abstract.
37. Francis CW, Onundarson PT, Carstensen EL, Blinc A, Meltzer RS, Schwarz K, Marder VJ. Enhancement of fibrinolysis in vitro by ultrasound. *J Clin Invest*. 1992;90:2063-2068.
38. Blinc A, Francis CW, Trudnowski JL, Carstensen EL. Characterization of ultrasound-potentiated fibrinolysis in vitro. *Blood*. 1993;81: 2636-2643.
39. Siddiqi F, Blinc A, Braaten J, Francis CW. Ultrasound increases flow through fibrin gels. *Thromb Haemost*. 1995;73:495-502.
40. Harpaz D, Chen X, Francis CW, Marder VJ, Meltzer RS. Ultrasound enhancement of thrombolysis and reperfusion in vitro. *J Am Coll Cardiol*. 1993;21:1507-1511.
41. Mizuno K, Satomura K, Miyamoto A, Arakawa K, Shibuya T, Arai T, Kurita A, Nakamura H, Ambrose JA. Angioscopic evaluation of coronary-artery thrombi in acute coronary syndromes. *N Engl J Med*. 1992;326:287-291.
42. Ambrose JA, Alexopoulos D. Thrombolysis in unstable angina: will the beneficial effects of thrombolytic therapy in myocardial infarction apply to patients with unstable angina? *J Am Coll Cardiol*. 1989; 13:1661-1671.
43. Uchida Y, Masuo M, Tomaru T, Kato A, Sugimoto T. Fiberoptic observation of thrombosis and thrombolysis in isolated human coronary arteries. *Am Heart J*. 1986;112:691-696.
44. Hess H, Ingrisch H, Mietaschk T, Rath H. Local low-dose thrombolytic therapy of peripheral arterial occlusions. *N Engl J Med*. 1982;307:1627-1636.
45. McNamara TO, Fischer JR. Thrombolysis of peripheral arterial and graft occlusion. *Am J Radiol*. 1985;144:769-775.
46. Semba CP, Dake MD. Iliofemoral deep venous thrombosis: aggressive therapy with catheter-directed thrombolysis. *Radiology*. 1994; 191:487-494.
47. Voter WA, Lucaveche C, Erickson HP. Concentration of protein in fibrin fibers and fibrinogen polymers determined by refractive index matching. *Biopolymers*. 1986;25:2375-2384.
48. Press WH, Teukolsky SA, Vetterling WT, Flannery BP. *Numerical Recipes in C: The Art of Scientific Computing*. 2nd ed. Cambridge, UK: Cambridge University Press; 1992.
49. Booth NA, Robbie LA, Croll AM, Bennett B. Lysis of platelet-rich thrombi: the role of PAI-1. *Ann N Y Acad Sci*. 1992;667:70-80.
50. Brommer EJP, Potter van Loon, BJ, Rijken DC, Van Bockel JH. Composition and susceptibility to thrombolysis of pathological human arterial thrombi. *Ann N Y Acad Sci*. 1992;667:283-285.
51. Thorsen S, Mullertz S, Suenson E, Kok P. Sequence of formation of molecular forms of plasminogen and plasmin-inhibitor complexes in plasma activated by urokinase or tissue-type plasminogen activator. *Eur J Biochem*. 1984;223:179-187.
52. Husain SS, Hasan AAK, Budzynski AZ. Differences between binding of one-chain and two-chain tissue plasminogen activators to non-cross-linked and cross-linked fibrin clots. *Blood*. 1989;74:999-1006.
53. Zamarron C, Lijnen HR, Collen D. Kinetics of the activation of plasminogen by natural and recombinant tissue type plasminogen activator. *J Biol Chem*. 1984;259:2080-2093.
54. Collen D, Zamarron C, Lijnen HR, Hoylaerts M. Activation of plasminogen by pro-urokinase. *J Biol Chem*. 1986;261:1259-1266.
55. Lottenberg R, Christensen U, Jackson CM, Coleman PL. Assay of coagulation proteases using peptide chromogenic and fluorogenic substrates. *Methods Enzymol*. 1981;80:341-361.
56. Wu JH, Diamond SL. A fluorescence quench and dequench assay of fibrinogen polymerization, fibrinogenolysis, and fibrinolysis. *Anal Biochem*. 1995;224:83-91.
57. Wiman B, Collen D. On the kinetics of the reaction between human antiplasmin and plasmin. *Eur J Biochem*. 1978;84:573-578.
58. Virca GD, Travis J. Kinetics of association of human proteinases with human α_2-macroglobulin. *J Biol Chem*. 1984;259:8870-8878.
59. Lijnen HR, Van Hoef B, Collen D. On the reversible interaction of plasminogen activator inhibitor-1 with tissue-type plasminogen activator and with urokinase-type plasminogen activator. *J Biol Chem*. 1991;266:4041-4044.
60. Wiman B, Lijnen HR, Collen D. On the specific interaction between the lysine-binding sites in plasmin and complementary sites in a2-antiplasmin and in fibrinogen. *Biochim Biophys Acta*. 1979;579:142-154.